International Journal of General Medicine

Dovepress
Taylor & Francis Group

Open Access Full Text Article

ORIGINAL RESEARCH

Very-High-Frequency Ultrasonographic Profiling Characteristics of Nodular Hidradenoma: A Retrospective Analysis

Bin Dong[1], Hongsheng Xia[1], Ying Liu[2], Su Wang[3], Zhubiao Ye[4]

[1]Department of Ultrasound, Hangzhou Third People's Hospital, Hangzhou Third Hospital Affiliated to Zhejiang Chinese Medical University, Hangzhou, People's Republic of China; [2]Department of Ultrasound Medicine, Zhejiang Provincial People's Hospital (Affiliated People's Hospital), Hangzhou Medical College, Hangzhou, People's Republic of China; [3]Department of Dermatology, Haining Maternity and Child Health Care Hospital, Haining, People's Republic of China; [4]Department of Dermatology, Hangzhou Third People's Hospital, Hangzhou Third Hospital Affiliated to Zhejiang Chinese Medical University, Hangzhou, People's Republic of China

Correspondence: Zhubiao Ye, Department of Dermatology, Hangzhou Third People's Hospital, Hangzhou Third Hospital Affiliated to Zhejiang Chinese Medical University, West Lake Road 38, Hangzhou, 310009, People's Republic of China, Email yyis9447@126.com

Background: Nodular hidradenoma (NH) is a rare benign adnexal tumor originating from sweat glands, often misdiagnosed due to nonspecific clinical manifestations. Ultrasonography (US) plays a critical role in the diagnosis of skin tumors, yet systematic descriptions of its sonographic features remain limited.

Objective: This study aims to investigate the very-high-frequency (VHF) characteristics of eccrine nodular hidradenoma (ENH) and establish key imaging criteria to differentiate it from other cutaneous/subcutaneous lesions.

Methods: A retrospective analysis was conducted on 32 histopathologically confirmed ENH cases between November 2018 and December 2024. The VHF ultrasound evaluated ENH location, size, shape, margin, boundary, echogenicity, calcification, blood supply, and so on.

Results: The VHF features of ENH showed that the maximum diameter of the lesions was about 12.42 ± 7.66 mm. Most lesions revealed predominant craniofacial/limb involvement (62.5%) and almost all lesions (96.9%) demonstrated transdermal extension into subcutaneous tissue. Lesion morphology varied from geometric regularity (87.5%) to irregular lobulation (12.5%), reflecting ENH's structural diversity. Echogenicity patterns were classified as: homogeneous solid hypoechoic architecture (6.2%, 2/32), heterogeneous solid-dominant hypoechogenicity (40.6%, 13/32), mixed echogenicity with solid-cystic components (31.3%, 10/32, solid:cystic ≈1:1), mixed cystic-dominant echogenicity (21.9%, 7/32). Notably, the ultrasound features of inner septa, "snow falling" or "fluid-fluid level" were observed in some lesions. Additionally, 9.4% (3/32) showed intralesional calcifications and all lesions exhibited posterior acoustic enhancement. Doppler analysis highlighted vascular heterogeneity, with 87.5% (28/32) classified as Adler grade 2–3, correlating histopathologically with vascularized stromal septa.

Conclusion: The VHF ultrasound demonstrates characteristic diagnostic features of ENH, including its anatomical predilection, the involved skin layers, heterogeneous internal echogenicity, and distinctive blood flow patterns. These features provide critical indicators for differential diagnosis, establishing VHF ultrasound as a pivotal imaging modality to enhance diagnostic precision and optimize clinical decision-making in dermatologic oncology.

Keywords: Eccrine nodular hidradenoma, very-high-frequency ultrasound, diagnosis

Introduction

Eccrine nodular hidradenoma (ENH), a rare benign adnexal tumor arising from the eccrine sweat glands, is characterized by its histopathological complexity and clinical diagnostic challenges.[1] Typically presenting as a solitary, slow-growing, and asymptomatic subcutaneous nodule, ENH predominantly affects the extremities and trunk in middle-aged adults.[2] Primary lesions often exhibit intact or ulcerated surfaces with chromatic variations ranging from flesh-toned to bluish pigmentation. Secondary changes, including erosion, bleeding, or rapid enlargement, are occasionally reported in cases mimicking malignancy.[3,4] The differentiation

Received: 11 May 2025
Accepted: 27 August 2025
Published: 4 September 2025

of hidradenoma from other cutaneous tumors remains challenging when relying solely on clinical observation of skin lesions without utilizing imaging or histopathological techniques.[5] Despite its benign nature, ENH may mimic malignant lesions (eg, metastatic carcinoma or melanoma) due to overlapping clinical features, leading to unnecessary invasive interventions.[3,4]

Histologically, nodular hidradenoma may exhibit differentiation features toward either eccrine or apocrine sweat glands, exhibiting a biphasic cellular architecture characterized by polygonal epithelial cells and duct-like differentiation accompanied by solid-cystic changes.[1] Previous studies have reported that apocrine-differentiated nodular hidradenomas demonstrate higher prevalence compared to their eccrine counterparts, resulting in predominant research focus on apocrine variants through both imaging and histopathological investigations,[6] while eccrine-derived hidradenomas remain less frequently documented.

As a convenient and non-invasive diagnostic modality, very high-frequency (VHF) ultrasound with exceptionally high resolution has emerged as a valuable imaging tool for distinguishing characteristic features among various cutaneous neoplasms.[7] Previous studies have delineated the sonographic characteristics of apocrine-derived hidradenomas as follows:[6] heterogeneously hypoechoic architecture (encompassing distinctive features such as the "snow falling sign" and "fluid-fluid level") in conjunction with posterior acoustic enhancement, reflecting coexisting solid and cystic components. Despite these advancements, the literature remains remarkably scarce regarding detailed ultrasonographic descriptions of eccrine-originated hidradenomas, substantially limiting their clinical differentiation.

To address this gap, we systematically reviewed and comprehensively analyzed the sonographic features of 32 histopathologically confirmed ENH cases. This study aims to enhance dermatologists' and radiologists' understanding of ultrasonographic manifestations specific to eccrine nodular hidradenomas, thereby facilitating improved differentiation from other cutaneous tumors and enabling earlier, more precise diagnostic decision-making.

Materials and Methods

Study Population

This retrospective study enrolled 32 patients with eccrine nodular hidradenoma (ENH) (16 males, 16 females; age range: 10–79 years; mean age: 50.25 ± 15.14 years) who were admitted to Hangzhou Third People's Hospital (Hangzhou, China) between November 2018 and December 2024. All participants were of Chinese nationality. All cases were pathologically confirmed through excisional biopsy, with exclusion criteria applied to patients with ambiguous histopathological diagnoses or concurrent cutaneous malignancies. Demographic and clinical characteristics, including lesion location and skin involvement patterns, were systematically documented (Table 1).

Table 1 VHF Ultrasound Features of ENH

	ENH, n=32
Gender	
Male	16
Female	16
Age (years)	50.25 ± 15.14
Lesion size (mm)	
Maximum diameter	12.42 ± 7.66
Shape	
Regular	28
Lobulated	4

(*Continued*)

Table 1 (Continued).

	ENH, n=32
Location	
Dermis	1
Dermis and hypodermis	31
Composition	
Solid	2
Solid + cystic (cystic < 20%)	13
Solid + cystic (1: 1)	10
Solid + cystic (cystic > 80%)	7
Internal structures	
Inner septa	7
Snow falling sign	1
Fluid-fluid level	3
Doppler signal	
Grade 1	4
Grade 2	15
Grade 3	13

Histopathological Processing Protocol

Excised specimens were immediately fixed in 10% neutral buffered formalin for 24–48 hours. Fixed tissues underwent standardized dehydration through graded ethanol series (70%-100%), xylene clearing, and paraffin embedding. Serial 4-μm sections were stained with hematoxylin and eosin (H&E) using the Shandon Varistain Gemini protocol.

Ultrasound Imaging Protocol

High-resolution ultrasonography was performed using the Esaote MyLab™ One (Italy) color Doppler system equipped with a 22 MHz ultra-high-frequency linear probe. Each lesion was evaluated in both maximum diameter and thickness, with particular attention to morphological features: Lesion localization: Precise anatomical mapping relative to skin layers (epidermis, dermis, hypodermis). Morphological descriptors: Size (maximum diameter, thickness), shape (oval, lobulated, or irregular), margin definition (well-circumscribed vs infiltrative), composition (solid, solid + cystic, cystic), echogenicity (hypoechoic, mixed echoic, anechoic). Internal architecture: Analysis of echotexture homogeneity, presence of cystic spaces, calcifications, or hyperechoic linear structures. Vascularity: Semi-quantitative assessment via color Doppler (Adler's grading: 0–3) to categorize blood supply patterns. Two board-certified dermatologists with >5 years of specialized experience in cutaneous ultrasound independently reviewed all images. Ultrasonographic findings were systematically cataloged using a predefined checklist to ensure standardized reporting.

Ethical Compliance

The study protocol received approval from the Institutional Ethics Committee of Hangzhou Third People's Hospital (Approval No: 2025KA115). Prior to participation, written informed consent was obtained from all patients or legal guardians for the anonymized publication of clinical images, with explicit emphasis on voluntary participation and data confidentiality.

Statistical Considerations

Descriptive statistics (mean ± SD, frequency distributions) were applied to demographic and sonographic variables.

Results

The retrospective analysis included 32 patients (16 females, 16 males; mean age 50.25 ± 15.14 years) diagnosed with ENH. Anatomical distribution analysis revealed lesions across 15 body regions, with lesions documented in the scalp (n=4), forehead (n=2), nose (n=1), lip (n=4), face (n=4), neck (n=1), shoulders (n=2), axilla (n=1), back (n=1), abdomen (n=1), vulva (n=1), gluteal region (n=1), inguinal area (n=1), upper extremities (n=3), and lower extremities (n=5). Of particular note, the craniofacial region (head/face) and limbs demonstrated a predilection for lesion development, collectively accounting for 62.5% of total cases (20/32), whereas other sites showed limited involvement. Ultrasonographic evaluation demonstrated two distinct patterns of dermal-subcutaneous involvement: superficial dermal localization (n=1, 3.1%) and transdermal extension into the subcutaneous layer (n=31, 96.9%). The dataset offers a thorough examination of cutaneous layer involvement patterns across the sampled population. The cohort demonstrated a spectrum of enhancement patterns, where lesion sizes varied between 5.2×4.7 mm and 43×32 mm, with 87.5% of lesions falling within 6–20 mm range. All cases demonstrated well-demarcated lesion margins. Morphological analysis revealed 87.5% (28/32) of lesions maintained geometric regularity, while 12.5% (4/32) displayed irregular lobulated contours, reflecting significant shape polymorphism. These quantitative parameters are systematically tabulated in the demographic-clinical matrix (Table 1), with the lower segment specifically detailing lesional characteristics.

Table 1 also shows the statistics of typical ENH lesions with different internal echoes. Ultrasonographic evaluation of 32 lesions revealed a heterogeneous spectrum of echogenic patterns: 2 lesions (2/32, 6.2%) demonstrated homogeneous solid hypoechoic structure (Figure 1), 13 lesions (13/32, 40.6%) exhibited heterogeneous hypoechogenicity, solid-

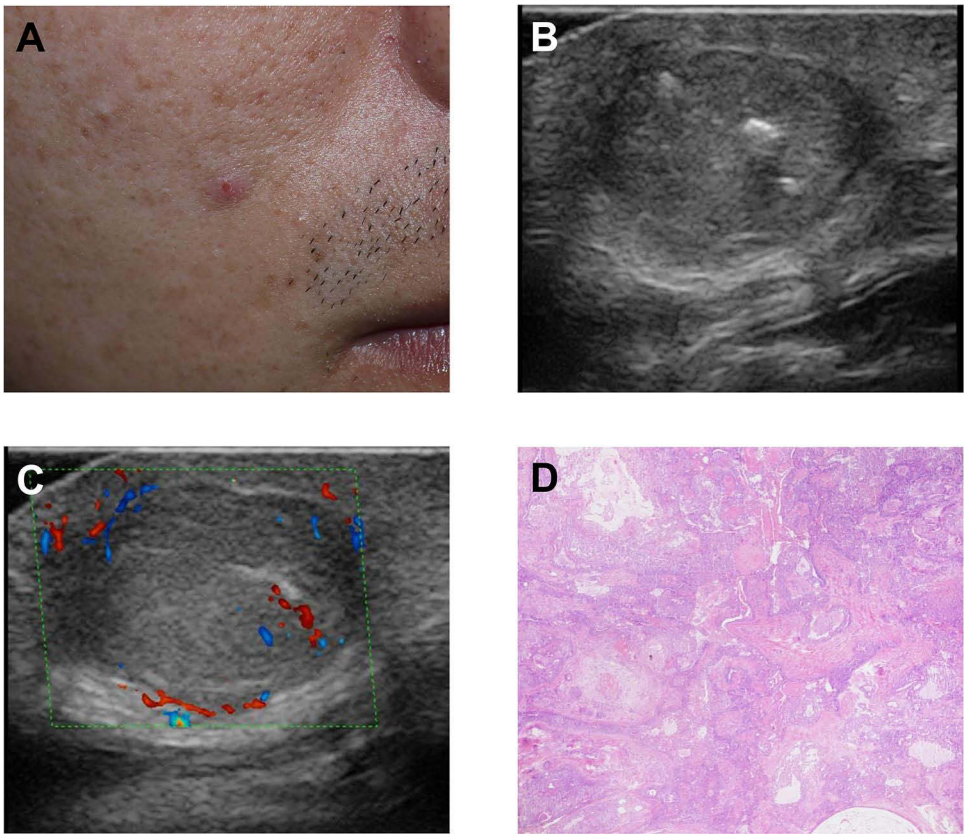

Figure 1 Multimodal characterization of eccrine nodular hidradenoma (ENH) in a 35-year-old male. (**A**) Clinical presentation of a nodular lesion on the lower lip vermilion border. (**B**) B-mode ultrasonography demonstrates a transdermal hypoechoic mass infiltrating subcutaneous adipose tissue, containing a calcific focus. (**C**) Color Doppler reveals moderate vascularity (Grade 2) with confluent signals in <50% of the solid component. (**D**) The histopathological features were diagnostic of nodular hidradenoma with eccrine differentiation (hematoxylin and eosin [H&E] stain, original magnification ×20).

dominant internal components with scattered microcystic areas (cystic < 20%) (Figure 2). 10 lesions (10/32, 31.3%) displayed mixed echogenicity with approximately equal proportions of solid (50%) and cystic (50%) components. Notably, "fluid-fluid level" sign were present in this group of cases (Figure 3). 7 lesions (7/32, 21.9%) displayed mixed echogenicity manifested cystic-dominant masses with papillary solid projections (cystic > 80%) (Figure 4). The ultrasound features of inner septa, "snow falling" sign, and fluid-fluid level were also observed in ENH (Figure 5). This

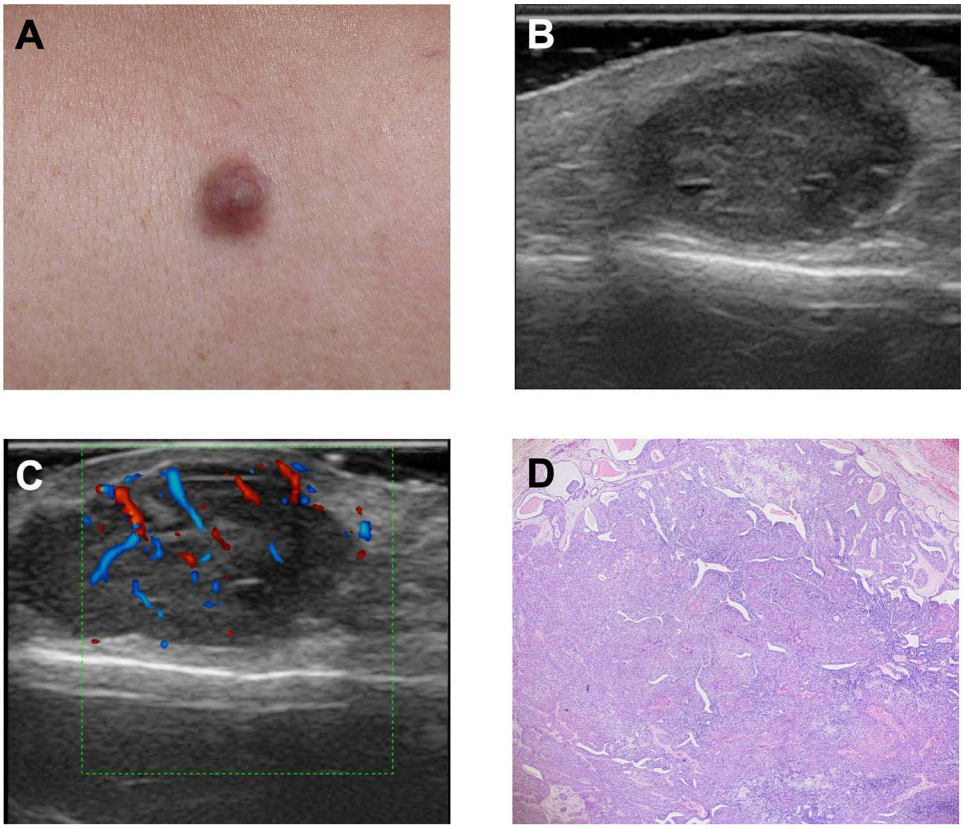

Figure 2 Multiple characteristics of ENH in a 55-year-old woman. (**A**) Clinical photograph of the lesion on her back. (**B**) The B mode VHF image shows a well-defined regular cystic + solid (cystic < 20%) lesion invaded the dermis and subcutaneous fat layer. The lesion displayed heterogeneous hypoechogenicity, small cystic areas were also seen within the lesion. (**C**) Color Doppler sonogram showed confluent color signals are present in more than half of the solid component (Grade 3). (**D**) Immunohistochemical analysis demonstrated ductal differentiation patterns characteristic of eccrine-origin nodular hidradenoma (hematoxylin and eosin [H&E] stain, original magnification ×20).

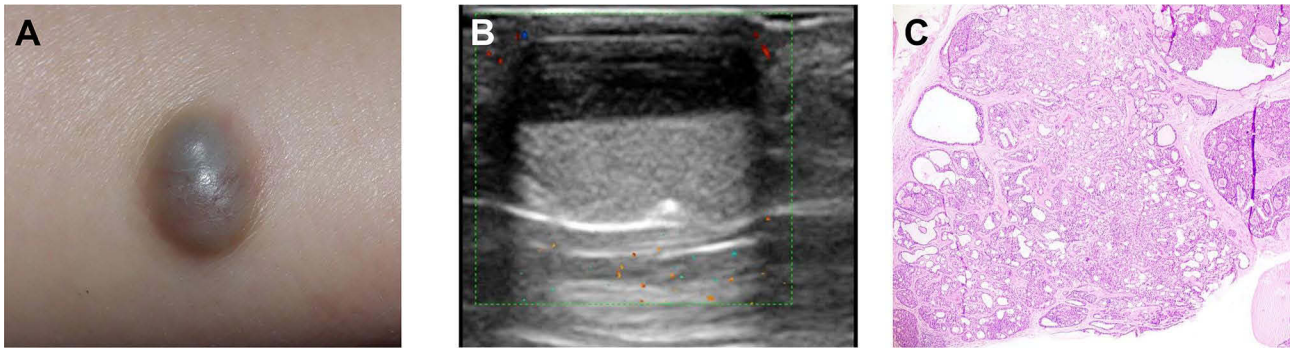

Figure 3 Multimodal features of ENH in a 40-year-old female. (**A**) Clinical presentation demonstrating an upper limb lesion. (**B**) VHF ultrasound image reveals a well-circumscribed, ovoid lesion with equal cystic and solid components (1:1 ratio) extending into the dermis and subcutaneous adipose tissue. The mass exhibits heterogeneously mixed echogenicity with an internal "fluid-fluid level" sign. Color Doppler imaging demonstrates moderate vascularity (<50% parenchymal involvement, Grade 2) within the solid portion. (**C**) Histopathological confirmation showing characteristic ductal structures and epithelial cell proliferation (hematoxylin and eosin [H&E] stain, original magnification ×20).

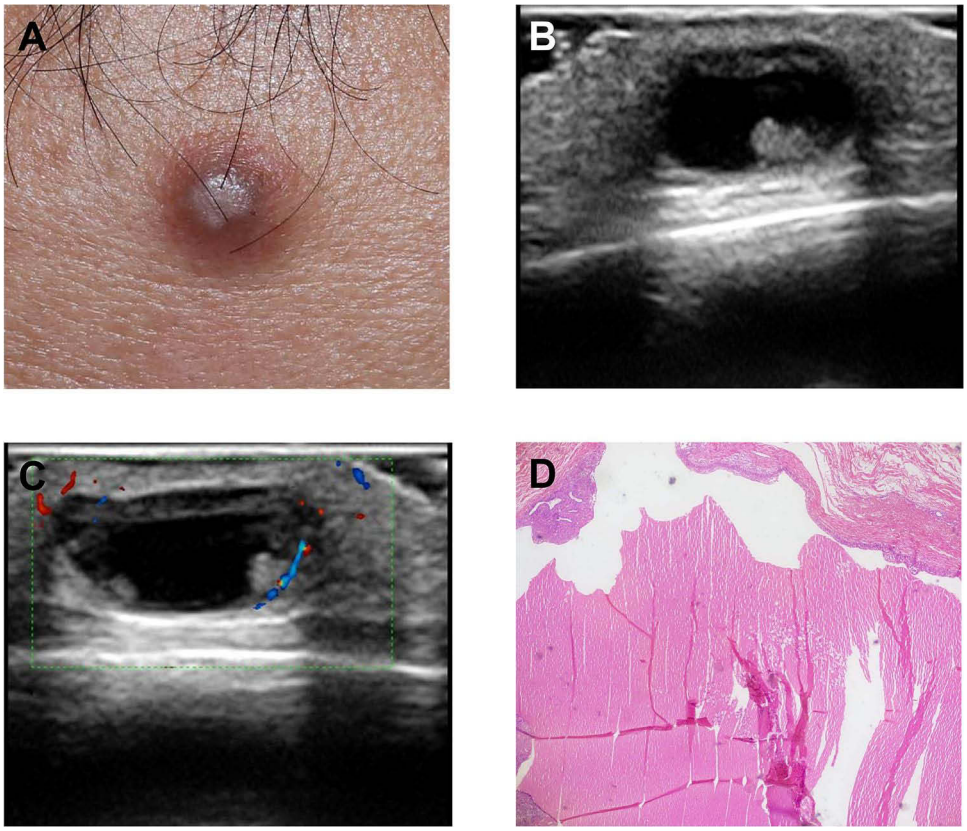

Figure 4 Diagnostic features of ENH in a 39-year-old male. (**A**) Clinical presentation of a forehead lesion. (**B**) B-mode VHF ultrasound demonstrates a well-circumscribed, predominantly cystic (cystic > 80%) lesion extending into the dermis and subcutaneous adipose tissue, displaying heterogeneously mixed echogenicity. (**C**) Color Doppler imaging reveals moderate vascularity (Grade 2: <50% parenchymal involvement) within the solid component. (**D**), Histopathological examination confirms lobular architecture with characteristic ductal differentiation (hematoxylin and eosin [H&E] stain, original magnification ×20).

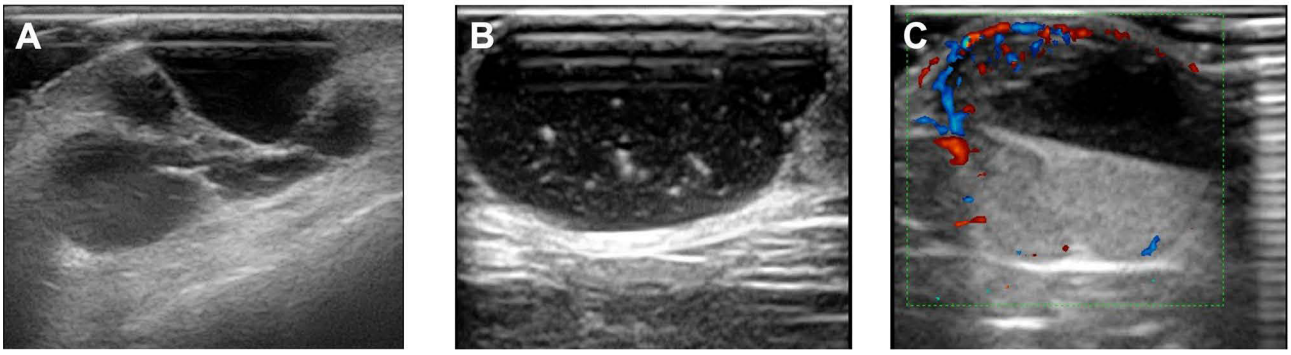

Figure 5 The VHF ultrasound features of ENH. (**A**) Inner septa. (**B**) "Snow falling" sign. (**C**) "fluid-fluid level" sign.

continuum of sonographic features purely solid, complex cystic-solid, and microcystic architectures highlights the diverse structural complexity of ENH. Additionally, three (3/32, 9.4%) lesions demonstrated intralesional calcifications, while all lesions with posterior acoustic enhancement.

The Doppler evaluation of 32 hidradenomas demonstrated significant vascular heterogeneity, with Adler blood flow grading revealing the following distribution (Table 1): 4 cases (4/32, 12.5%) exhibited grade 1 (minimal vascularity), 15 cases (15/32, 46.9%) displayed grade 2 (moderate vascularity with 1–2 vessel clusters), and 13 cases (13/32, 40.6%) showed grade 3 (marked vascularity with ≥3 vessel clusters or diffuse flow). Notably, the high prevalence of Adler grade

2–3 lesions (87.5% combined) aligns with the histopathological features of hidradenomas, which often contain vascularized stromal septa and papillary projections.

Discussion

Eccrine nodular hidradenoma manifests as a single, gradually enlarging, symptom-free lesion (0.5–3 cm diameter) with diverse cutaneous presentations including intact, thickened, or eroded surfaces displaying chromatic variations from flesh-toned to bluish pigmentation.[8] Histopathological analysis reveals distinctly bordered tumor masses containing polygonal acidophilic and vacuolated cells organized in compact arrangements, featuring characteristic glandular structures and fluid-filled cavities within the dermal layers.[9]

Based on the analysis of 32 surgically confirmed eccrine nodular hidradenoma lesions, our study systematically characterized the sonographic features of these tumors. To the best of our knowledge, these cases represent the largest documented series of ENH in ultrasonographic studies and may provide diagnostic tools to support its distinct preliminary differentiation from other dermatologic entities. Our analysis of 32 ENH cases demonstrated transdermal extension into subcutaneous tissue in 96.9% (31/32) of lesions, with only 3.1% (1/32) localized to the superficial dermis, mirroring findings from previous studies.[6,10] This aligns with ENH's histopathological origin from eccrine sweat glands, which predominantly reside at the dermal-subcutaneous junction. The transdermal growth pattern observed in nearly all cases underscores ENH's tendency to infiltrate deeper skin layers, a critical diagnostic marker differentiating it from purely epidermal lesions (eg, epidermal cysts). Notably, 100% (32/32) of lesions maintained well-demarcated margins despite their subcutaneous extension, reflecting their benign yet locally invasive nature. A striking finding in our series was the universal presence of posterior acoustic enhancement (32/32, 100%), a feature not previously reported in ENH literature.[10] Our data revealed a craniofacial/limb predilection (62.5%, 20/32), with lower extremities (15.6%, 5/32) and lips (12.5%, 4/32) being frequent sites, whereas previous studies did not perform statistical analysis.[6,10] This distribution correlates with eccrine gland density, which peaks in acral regions. However, 9.4% (3/32) presented at atypical sites (vulva, gluteal, inguinal), expanding ENH's known topographic spectrum. Compared to prior studies reporting trunk dominance in apocrine hidradenomas, our findings highlight ENH's distinct anatomic bias, likely reflecting eccrine gland embryologic distribution. Vascularity assessment detected moderate intralesional blood flow (Adler grade 1–3) in every lesion, contrasting with the typically avascular appearance of benign epidermal cysts. These observations-deep transdermal infiltration, universal posterior enhancement, craniofacial/limb predilection and blood flow patterns-provide a diagnostic triad for ENH.

The sonographic heterogeneity observed in ENH aligns with their intrinsic histopathological complexity. ENH's biphasic histopathology—solid epithelial nests interspersed with ductal structures and cystic cavities—directly informs its sonographic heterogeneity. The polygonal cell clusters manifest as solid hypoechoic regions, while ductal lumina containing eosinophilic secretions correlate with microcystic components. This structural duality explains the spectrum from purely solid to cystic-dominant echogenic patterns observed in our cohort. Our findings demonstrate that ENH predominantly manifests as mixed echogenicity (variable solid-to-cystic ratios or cystic dominant architecture), followed by heterogeneous solid-dominant hypoechogenicity, and homogeneous hypoechogenicity, which is not completely consistent with previous study reported by Feng MC et al.[10] This variation may be attributed to interobserver variability in the classification criteria for solid-cystic ratios and/or technical differences in ultrasound system parameters, particularly the operational frequency ranges of transducers, which influence spatial resolution and tissue contrast.[11] Notably, the 9.4% incidence of calcifications may correlate with reactive fibroplasia and chronic perilesional inflammation-a hypothesis supported by histopathological studies linking dystrophic calcifications to stromal remodeling in adnexal tumors.

The identification of internal septations, "snow falling" sign, or "fluid-fluid level" sign on ultrasound further corroborates earlier descriptions of ENH as lesions with compartmentalized cystic and solid components. These features are directly influenced by the proportion of cystic-to-solid elements: septations arise from fibrous bands partitioning cystic cavities, while fluid-fluid levels indicate sedimentation of proteinaceous debris or hemorrhage within cystic spaces. Such morphological markers not only enhance diagnostic specificity but also provide preoperative insights into lesion architecture, aiding surgical planning to minimize collateral tissue damage.

A striking observation in our study is the universal presence of posterior acoustic enhancement across all ENH lesions, rarely emphasized in prior literature This phenomenon may stem from two synergistic mechanisms: (1) microstructural

complexity within the tumor (eg, alternating cystic and solid regions) causing constructive interference of backscattered ultrasound waves, and (2) acoustic impedance mismatch at the lesion-periphery interface, where abrupt transitions between dense cellular clusters and loose stroma amplify signal transmission. This contrasts with malignant cutaneous tumors (eg, melanomas), which often exhibit posterior shadowing due to dense cellular packing and high collagen content, suggesting that posterior enhancement could serve as a differential diagnostic marker.[12]

This study has two primary limitations: the cohort was restricted to a Chinese population (representing a single ethnic group), and the relatively small sample size (n=32), both of which may affect the generalizability of the findings. However, this constraint is inherent to the rarity of sweat gland-derived tumors compared to other cutaneous lesions. Nevertheless, our findings suggest that ultrasonographic evaluation could reduce clinical and dermoscopic misdiagnosis and potentially differentiate these lesions from malignant skin tumors.

Further research is warranted to validate the observed ultrasonographic morphological features by comparing them with larger cohorts, particularly focusing on apocrine or eccrine variants of nodular hidradenomas. Additionally, integrating histopathological correlation with imaging data could enhance diagnostic accuracy. The anatomical details provided by ultrasound may also improve cosmetic prognostication by enabling precise preoperative planning, such as minimizing resection margins while ensuring complete tumor excision. Future studies should explore the utility of standardized ultrasonographic criteria in guiding both diagnostic and therapeutic decision-making for these uncommon adnexal neoplasms.

Conclusions

In summary, our analysis of eccrine variants revealed both overlapping and distinct sonographic features. While shared characteristics encompass dermal-subcutaneous localization, heterogeneous solid-cystic echotexture, Adler blood flow grading, and hallmark features such as inner septa, the snowfall sign, and fluid-fluid levels, this study identifies two critical discriminators for ENH: (1) universal posterior acoustic enhancement; and (2) craniofacial/limb predilection. These distinctions, particularly the pathognomonic posterior acoustic enhancement, address a key diagnostic gap by differentiating ENH from malignant mimics (eg, melanomas exhibiting posterior shadowing). The proposed imaging criteria—combining anatomical distribution, lesional architecture, and enhancement patterns—provide a structured framework to reduce diagnostic ambiguity in clinical practice.

Data Sharing Statement

The datasets generated in this study can be obtained from the corresponding author upon formal request.

Ethics Approval and Informed Consent

This study was conducted in accordance with the Declaration of Helsinki. Ethics approval was granted by the Hangzhou Third People's Hospital ethics committee (2025KA115). All participants provided written informed consent prior to their participation.

Funding

The authors declare that no funds, grants, or other financial support were received during the preparation of this manuscript.

Disclosure

The authors disclose that they have no competing interests for this work.

References

1. Correia C, De Vasconcelos P, Soares-de-Almeida L. Nodular hidradenoma: clinical, dermoscopic, and histopathological features. *Dermatol Online J*. 2024;30(2). doi:10.5070/D330263594
2. Robles-Mendez JC, Martinez-Cabriales SA, Villarreal-Martinez A, et al. Nodular hidradenoma: dermoscopic presentation. *J Am Acad Dermatol*. 2017;76(2S1):S46–S48. doi:10.1016/j.jaad.2016.07.003
3. Yan M, Gilmore H, Harbhajanka A. Low-Grade Mucoepidermoid Carcinoma Versus Nodular Hidradenoma: potential Diagnostic Challenge in Breast Pathology. *Int J Surg Pathol*. 2021;29(3):346–347. doi:10.1177/1066896920981635

4. Punia RP, Garg S, Bal A, Mohan H. Pigmented nodular hidradenoma masquerading as nodular malignant melanoma. *Dermatol Online J*. 2008;14 (1):15. doi:10.5070/D38R0187N1
5. Shalini B, Akshi K, Namrata N, Shilpi S, Manupriya N. Case of chondroid syringoma mimicking a nodular hidradenoma: a diagnostic pitfall on cytopathology. *Diagn Cytopathol*. 2018;46(1):59–62. doi:10.1002/dc.23791
6. Wortsman X, Reyes C, Ferreira-Wortsman C, Uribe A, Misad C, Gonzalez S. Sonographic Characteristics of Apocrine Nodular Hidradenoma of the Skin. *J Ultrasound Med*. 2018;37(3):793–801. doi:10.1002/jum.14379
7. Dinnes J, Bamber J, Chuchu N, et al. High-frequency ultrasound for diagnosing skin cancer in adults. *Cochrane Database Syst Rev*. 2018;12(12): CD013188. doi:10.1002/14651858.CD013188
8. Bijou W, Laababsi R, Oukessou Y, et al. An unusual presentation of a nodular hidradenoma: a case report and review of the literature. *Ann Med Surg (Lond)*. 2021;61:61–63. doi:10.1016/j.amsu.2020.11.050
9. Nandeesh BN, Rajalakshmi T. A study of histopathologic spectrum of nodular hidradenoma. *Am J Dermatopathol*. 2012;34(5):461–470. doi:10.1097/DAD.0b013e31821a4d33
10. Feng MC, Liang JF, Wang J, Dai JC, Xu WM. Ultrasound Features of Nodular Hidradenoma: a Case Series of 27 Patients. *J Ultrasound Med*. 2024;43(12):2411–2417. doi:10.1002/jum.16569
11. Mitsui Y, Ogawa K, Koga K, et al. Trichilemmal cysts with proteinaceous material: a potential diagnostic pitfall. *J Cutan Pathol*. 2022;49 (6):515–524. doi:10.1111/cup.14214
12. Russo A, Patane V, Gagliardi F, et al. Preliminary Experience in Ultra-High Frequency Ultrasound Assessment of Cutaneous Primary Lymphomas: an Innovative Classification. *Cancers (Basel)*. 2024;16(13):2456. doi:10.3390/cancers16132456